NeuroImage: Clinical 36 (2022) 103247

Contents lists available at ScienceDirect

NeuroImage: Clinical

journal homepage: www.elsevier.com/locate/ynicl

Multimodal imaging of essential tremor and dystonic tremor

Patrick Bédard [a,1], Pattamon Panyakaew [a,b,1], Hyun-Joo Cho [a], Mark Hallett [a], Silvina G. Horovitz [a,*]

[a] Human Motor Control Section, National Institute of Neurological Disorders and Stroke, National Institutes of Health, Bethesda, MD 20892-1428, USA
[b] Chulalongkorn Center of Excellence for Parkinson's Disease & Related Disorders, Department of Medicine, Faculty of Medicine, Chulalongkorn University and King Chulalongkorn Memorial Hospital, Thai Red Cross Society, Bangkok 10330, Thailand

ARTICLE INFO

Keywords:
Tremor
Essential tremor
Dystonic tremor
Neuroimaging

ABSTRACT

Despite recent advances in tremor and dystonia classification, it remains difficult to discriminate essential tremor from dystonic tremor as they are similar in appearance and no biomarker exists. Further, tremor can appear in the same or a different body part than the dystonia. The aim of the current study was to better understand the differential pathophysiology of these tremors.

We designed a cross-sectional case-control study and recruited 16 patients with essential tremor, 16 patients with dystonic tremor, and 17 age-matched healthy volunteers. We used multi-modal imaging combining resting-state functional MRI, diffusion tensor imaging, and magnetic resonance spectroscopy. We measured functional connectivity of resting-state fMRI to assess connectivity in the tremor network, fractional anisotropy and mean diffusivity with diffusion tensor imaging, and GABA+, Glutamate/Glutamine, Choline, and *N*-Acetylaspartate with spectroscopy (adjusted to Creatine).

Our results showed reduced functional connectivity of resting-state fMRI between the cerebellum and dentate nucleus bilaterally for the essential tremor group, but not the dystonic tremor group, compared to healthy volunteers. There was higher fractional anisotropy in the middle cerebellar peduncle bilaterally for the dystonic tremor group compared to the essential tremor group as well as for essential tremor group compared to healthy volunteers. There was also higher fractional anisotropy in the red nucleus and corticospinal tract for essential tremor and dystonic tremor groups compared to healthy volunteers. We also showed reduced mean diffusivity in the cerebellum of both essential tremor and dystonic tremor groups compared to healthy volunteers. Finally, we found elevated GABA+/Cr in the cerebellum of the essential tremor and dystonic tremor groups compared to healthy volunteers, but no difference emerged between essential tremor and dystonic tremor groups. We did not find group differences in the other metabolites.

Our results indicate cerebellar alterations in essential tremor and dystonic tremor patients compared to healthy volunteers, and further changes in the cerebellum network for the dystonic tremor patients. suggesting that the cerebellum is affected differently in both tremors.

1. Introduction

Tremor is one of the most prevalent features in movement disorders and occurs in Parkinson's disease and essential tremor (ET), but also in combination with other diseases such as dystonia, known as dystonic tremor (DT). Tremor is present in 14 to 86 % of dystonia patients while ET's prevalence is about 0.9 % in the general population (Pandey and Sarma, 2016; Louis and Faust, 2020b). While DT has its own classification (Deuschl et al., 1998; Albanese et al., 2013; Bhatia et al., 2018) it remains challenging to discriminate ET from DT and other tremor types since they look clinically similar, which impairs diagnosis and treatment.

A leading hypothesis of ET is the cerebellar neurodegeneration model centered on the Purkinje cells (PC) and neighboring neurons, which are GABAergic (Louis and Faust, 2020a). As a result of Purkinje cell loss, there is reduced inhibitory output towards the cerebellar nuclei which also have a decrease in $GABA_{A-B}$ receptors in the dentate nucleus (Paris-Robidas et al., 2012). Finally, this cascade of changes would

* Corresponding author.
E-mail address: silvina.horovitz@nih.gov (S.G. Horovitz).
[1] The first two authors contributed equally on this work.

https://doi.org/10.1016/j.nicl.2022.103247
Received 19 April 2022; Received in revised form 21 October 2022; Accepted 23 October 2022
Available online 25 October 2022

create a state of hyperexcitability resulting in tremor. The neuropathology of DT is not well understood yet, but dystonia neuropathology does involve the cerebellum (Prudente et al., 2013; Sharma, 2019).

Prior work, including that from our own lab, showed that DT differs from ET with more irregularities in tremor frequency and amplitude (Jedynak et al., 1991; Shaikh et al., 2008; Bove et al., 2018; Panyakaew et al., 2020) but others have reported similar oscillations between ET and DT (Rudzińska et al., 2013; Shaikh et al., 2015).

ET is usually considered a disease originating in the cerebellum while dystonia in basal ganglia, although both conditions clearly involve the cerebellum and broad brain networks (Lehéricy et al., 2013; Cerasa and Quattrone, 2016; Jinnah et al., 2017; Louis and Faust, 2020a). While numerous studies have shown cerebellar changes in ET and in other parts of the brain though less consistently (reviewed in Cerasa and Quattrone, 2016; Louis and Faust, 2020a), only a handful of studies have assessed brain correlates of DT (Cerasa et al., 2014; Kirke et al., 2017; Battistella and Simonyan, 2019; DeSimone et al., 2019; Hess et al., 2020; Sedov et al., 2020), and these varied regarding the type of dystonia patients recruited and methods used, preventing a broader understanding of DT. For example, a functional MRI study with a hand grip task showed reduced brain activation and connectivity in cerebellum, basal ganglia, sensorimotor cortex, and inferior parietal lobule for DT with cervical dystonia compared to ET (DeSimone et al., 2019). A study recorded pallidal neurons in cervical dystonia patients with jerky compared to sinusoidal tremor and showed different firing pattern depending on the tremor type (Sedov et al., 2020). A diffusion tensor imaging (DTI) study in patients with DT of voice and isolated spasmodic dysphonia reported fractional anisotropy difference between the two patients groups in the internal capsule and increased fractional anisotropy for both patients groups in the inferior frontal gyrus compared to controls (Kirke et al., 2017). Thus, much remains to be understood about the pathophysiology of ET, DT and how much do they share with each other.

Our primary objectives entail better understanding the pathophysiology of ET and DT and finding some brain characteristics to identify and distinguish DT from ET. While prior work on ET and DT mostly used unimodal imaging, here we used multimodal imaging approach, combining resting-state functional MRI to evaluate cerebello-cortical network integrity, diffusion tensor imaging (DTI) to evaluate integrity of the white and grey matter, and magnetic resonance spectroscopy (MRS) to measure changes in GABA and other metabolites in patients with DT and ET, and healthy controls. We also restricted the analysis to the tremor network (Haubenberger and Hallett, 2018) containing the cortico–ponto–cerebello–thalamo–cortical loop and the Guillain–Mollaret triangle. Combining neuroimaging metrics should allow to better characterize ET and DT by taking advantages of the strength of each modality for a specific condition. In turn, this should lead to better diagnosis and treatments. We included a control group to allow identifying and understanding the directionality of changes that could be affected in one or both patient' groups.

Given that ET and DT are hyperkinetic movement disorders, we hypothesized that this overactivity within the tremor network would be captured by specific brain changes in our metrics. We should find enhanced white matter signal along the tremor network pathways (enhanced fractional anisotropy), as well, we should find reduced GABA in the cerebellar hemisphere due to the GABAergic PC neurodegeneration and thus reduced inhibitory cerebellar output. Also, neuronal changes of PC would reduce the output to the dentate nucleus and thus functional connectivity between these areas should be reduced.

2. Materials and methods

2.1. Participants

We recruited 62 participants of which 49 (including 16 ET, 16 DT, and 17 age-matched healthy volunteers) (HV; Table 1) completed the MRI portion of the protocol. Thirteen participants did not complete the MRI portion of the study (due to claustrophobia, technical issues, not clear diagnosis, or metal in the body). Patients are the same as reported in an earlier clinical neurophysiological study (Panyakaew et al., 2020). The ET group all had bilateral tremor in their hands. The DT group was composed of patients having pure DT (pDT) and tremor associated with dystonia (TAWD) (see Supplementary Table 1). The pDT group had dystonia and tremor in the same hand (writer's cramp with writing tremor) and the TAWD group had dystonia in their neck and tremor in their hand (cervical dystonia with hand tremor). In our previous work (Panyakaew et al., 2020), we could distinguish between these two subgroups, but here with MRI we cannot. Nevertheless, we will present the data of each subgroup in Supplemental material for all our metrics.

Table 1
Participant demographics.

Measures	Groups			Statistics
	HV	ET	DT	
n	17	16	16	
Age	55.6 ± 14	58.9 ± 9	59.5 ± 12	$p = 0.75$
Sex	9F	7F	7F	$\chi^2 = 0.38$ $p = 0.82$
Handedness (R/L)	17/0	12/4	14/2	$\chi^2 = 4.79$ $p = 0.09$
TETRAS ADL	–	22.1 ± 5	12.1 ± 7.0	$p = 0.0001$
TETRAS Perf	–	19.3 ± 6	13.0 ± 7	$p = 0.01$
TETRAS total	–	41.4 ± 10	25.0 ± 12.0	$p = 0.0003$
Tremor onset	–	26.6 + 16.9	36.8 ± 18.9	$p = 0.14$
Tremor duration	–	31.6 ± 14.3	22.1 ± 19.0	$p = 0.16$
Dystonia onset	–	–	43.9 ± 15.4	*NA*
Dystonia duration	–	–	15.0 ± 15.2	*NA*
FMS	–	0 ± 0	3.3 ± 1.7	*NA*
TWSTRS	–	0 ± 0	3.6 ± 4.8	*NA*

TETRAS: The Essential Tremor Rating Assessment Scale; ADL: Activities of Daily Living, Perf: Performance. FMS, Fahn-Marsden Dystonia Rating Scale; TWSTRS, Toronto Western Spasmodic Torticollis Rating Scale. L-R: Left-Right. All DT patients have tremor in their hand. DT includes pDT: hand dystonia and TAWD with cervical dystonia.

All participants had normal physical and neurological examinations (other than ET or DT) as well as a normal routine clinical MRI. Exclusion criteria included the presence of any neurological or psychiatric disorder and comorbid depression or anxiety, active alcohol or illicit drug use. All patients received their diagnosis by a neurologist expert in movement disorders at the National Institutes of Health according to the Consensus Statement on Classification of tremor and dystonia (Albanese et al., 2013). Only one pDT patient received botulinum toxin injections and was studied 3 months after the last injection. Patients who took symptomatic medications did not take those for at least 5 half-lives before the MRI session. Subjects were assessed for tremor and dystonia severity with The Essential Tremor Rating Assessment Scale (TETRAS) as well as the Fahn-Marsden Dystonia Rating Scale (FMS) and the Toronto Western Spasmodic Torticollis Rating Scale (TWSTRS). All participants gave written informed consent in accordance with the Combined Neuroscience Institutional Review Board of the National Institutes of Health.

2.2. Data acquisition

We collected all MR data with a 3T GE scanner (Discovery MR750) equipped with 32-channel head coil in the Nuclear Magnetic Resonance Center at the National Institutes of Health.

2.2.1. Resting state fMRI

Resting state fMRI allows for evaluation of functional networks. We acquired multi-echo T2*-weighted *EPI* with TR = 2 *sec*, TE = 15.5, 34.3, and 53.1 ms, image matrix = 64×64, flip angle: 70°, FoV: 240, voxel size 3.5×3.5×3.5 mm and acquired 272 whole-brain images. We told participants to keep their eyes closed, stay awake, and not to think about

anything specific.

2.2.2. DTI

Diffusion imaging allows for evaluating the integrity of brain tissue. We acquired T2-weighted diffusion images with TR = 6751.68 ms, TE = 79 ms, Flip angle = 90°, voxel size 2.5 mm isotropic, acceleration factor (ASSET) 2, b-values (volumes): b = 0 (10), intermediate b = 300 (10) and b = 1100 (60) s/mm2 and phase-encode direction anterior-posterior.

2.2.3. MRS

We acquired ^{1}H-MRS spectra to characterize the metabolites in a selected region of interest (ROI), the right cerebellum (Fig. 4B). The cerebellar ROI was placed in the center of the right cerebellum to include the dentate nucleus. We choose the cerebellum for its known involvement in tremor and dystonia and the right hemisphere as most individuals are right-handed.

The ROI was a 30×20×20 mm voxel, prescribed on the axial plane, avoiding CSF, thus large water contamination for the spectra, and voxels outside the brain. After performing a high order shimming, the spectrum quality was evaluated with a short (128 reps, 1 min 28 *sec*) acquisition using a gradient echo point-resolved spectroscopy sequence (PRESS; Bottomley (1984), Bottomley (1987)), with a TR of 3 *sec* and TE = 30 ms. We then acquired ^{1}H-MRS using a GABA editing sequence (Rothman et al., 1993) which is a gradient echo PRESS sequence, with TR = 1.5 *sec*, TE = 68 ms, FA = 90°, and additional pairs of editing pulses. We collected a total of 768 repetitions (376 interleaved pairs plus 16 water reference pulses), acquisition time: 19 min 12 *sec*. Full sequence details are included in (Tinaz et al., 2014).

2.2.4. Anatomical MRI

Structural images provide information about major abnormalities. They also allow for tissue parcellation to control for MRS voxel composition and registration of the rsfMRI and DTI. We acquired a high-resolution anatomical sagittal T1-weighted scan with TR = 7.664 ms, TE = 3.42 ms, TI = 424 ms, field of view = 100, FoV: 240×240 mm, matrix size: 256×256, flip angle = 7°, 176 slices, voxel size 1×1×1 mm. We also acquired an axial T2 fat-saturated scan with TR = 7.5 *sec*, TE = 100.74 ms, matrix size: 256×192, FoV: 240×180 mm2, flip angle = 90°, 62 slices, voxel size 0.9375×0.9375×2.5 mm.

2.3. Data analysis

2.3.1. Resting state fMRI

We used AFNI, to process anatomical and resting-state *EPI*. We used the afni_proc.py tool in AFNI to analyze the resting-state *EPI* timeseries that included averaging the timeseries across the three echoes, removing the first three volumes, despiking the timeseries, registering the *EPI* data to the anatomical scan, adjusting for slice timing offsets, motion correct these timeseries referring to the first image with rigid body transformations using cubic polynomial interpolation, and spatially blurred the timeseries with a 6 mm FWHM Gaussian kernel. We applied a band-pass filter 0.01–0.1 Hz and also used @ANATICOR to remove white matter signal from the timeseries to reduce scanner-related artifacts (Jo et al., 2010). We set the motion limit at 3 mm and removed volumes with >10 % of outliers as defined with 3dToutcount tool in AFNI. We also regressed out the demeaned and derivatives of head motion parameters. The anatomical and the *EPI* timeseries were transformed to the MNI template with affine transformations.

We selected ROI that belong to the tremor network (Haubenberger and Hallett, 2018). The tremor network (Fig. 1A) includes bilaterally the cerebellar lobules V and IV, dentate nucleus, pons, ventral intermediate nucleus (VIM), primary motor cortex (M1), red nucleus, and inferior olive (ION). Fig. 1A shows regions for only one set of anatomically connected ipsilateral/contralateral ROI for clarity, but the analysis was done bilaterally. For each ROI and participant, we extracted the timeseries, computed each ROI average time courses, computed the Pearson's correlation and applied Fisher's z-transform for group analysis. We only analyzed correlations between ROI that are anatomically connected, for example between M1 and pons, between pons and cerebellar lobule V and VI. We removed outliers per group as value(s) more than three scaled median absolute deviations (MAD) away from the median. For this analysis, we removed no more than one participant per group for all comparisons.

2.3.2. DTI

We used various tools in AFNI (Analysis of Functional NeuroImages software; https://afni.nimh.nih.gov Cox, 1996), FATCAT (Taylor and Saad, 2013), TORTOISE (https://tortoise.nibib.nih.gov; Pierpaoli et al., 2010; Irfanoglu et al., 2016) and FSL (https://fsl.fmrib.ox.ac.uk). The T2 was axialized with the fat_proc_axialize_anat tool in AFNI to the MNI template and the T1 was aligned to the T2 scan. We used DIFFPREP tool in TORTOISE on the DWI data to correct for head motion, eddy-currents, and *EPI* susceptibility distortion. Then, we registered all dataset using TORTOISE's DR-TAMAS to the most representative participant. We

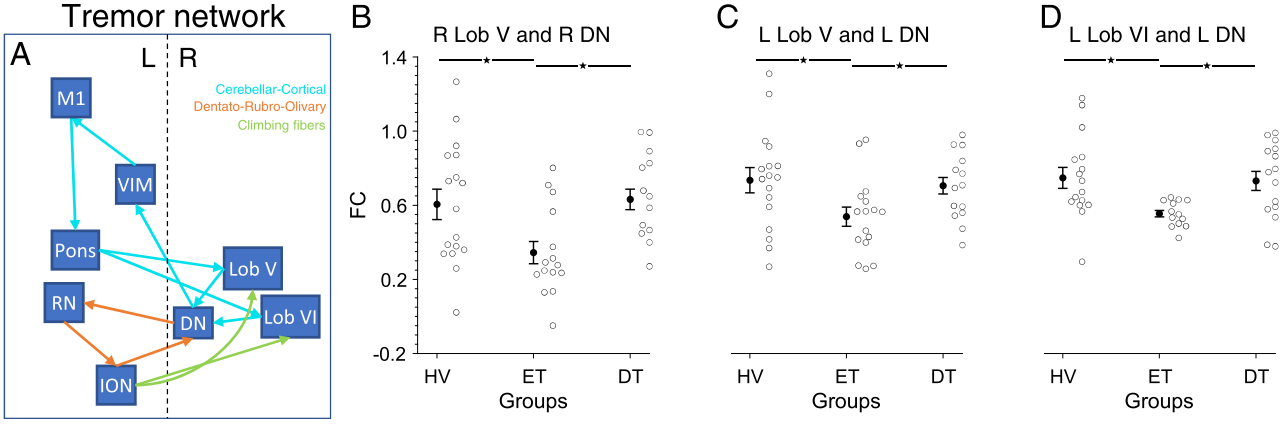

Fig. 1. Functional connectivity (FC) in the tremor network **A**: ROI of the tremor network; only one set of ipsilateral/contralateral ROI is shown for clarity, but the analysis was done bilaterally. **B-D**: Pair of ROI with significant main effect of Group ($p \leq 0.05$). Post-hoc *t*-test revealed significant differences between the ET and HV and DT who did not differ significantly from each other in 3 pairs of ROI. Dashed line is the midline, L-R: Left-Right, M1, primary motor cortex, ION: inferior olive nucleus, VIM: ventral intermediate thalamus, DN, dentate nucleus, Lob, lobule, RN, red nucleus. * $p \leq 0.05$. (For interpretation of the references to colour in this figure legend, the reader is referred to the web version of this article.)

computed fractional anisotropy (FA) and mean diffusivity (MD) with TORTOISE's DIFFCALC tool. We also transformed the data to the MNI template for better brain localization of significant clusters. For FA, we restricted the brain areas to the white matter within the tremor network with FA values >0.2, and for MD we also included the ROI themselves. Note that although iron content can impact DTI metrics (Pfefferbaum et al., 2010), it is unclear how iron content is affected in ET and DT.

We found no outliers to be removed.

2.3.3. MRS

We used an automated nonlinear fitting model run in IDL (ITT Visual Information Solutions, White Palins, NY, USA) as previously described (Geramita et al., 2011; Tinaz et al., 2014). Briefly, this model first removes the residual signal from water and fat using both the edited and unedited spectra. The choline (Cho), creatine (Cr), and *N*-Acetylaspartate (NAA) are then fitted from the unedited spectrum. The resulting fit is subtracted from the edited spectrum unmasking the GABA + peak at 3 ppm and allowing for fitting the GABA + signal, and glutamate and glutamine complex (Glx), which are then normalized to Cr.

To rule out effects of tissue composition, we computed the percentage of white matter, grey matter, and CFS for the right cerebellar ROI and compared across groups. Outliers removed were one HV and one ET for GABA and Glx, two HV and one ET for NAA, and one HV and three ET for Cho.

2.4. Statistical analysis

For MRS and functional connectivity we used ANOVA tool in R (R Core Team, 2021) and for DTI, we used the *randomize* tool in FSL. The *randomize* tool generates 5000 permutations to build the null distribution and implements a cluster thresholding using Threshold-Free Cluster Enhancement (Smith and Nichols, 2009). For MRS and functional connectivity, we used at $p \leq 0.05$, for DTI, we used a threshold free cluster enhancement of $p \leq 0.05$ as implemented in FSL. Then, in case of significant main effect of groups, we assessed groups differences with post-hoc pairwise two-tailed *t*-test and corrected for multiple comparisons with the False Discovery Rate approach (FDR; Benjamini and Hochberg, 1995) at $p \leq 0.05$. For all our ANOVAs, we assessed homogeneity of variance across groups with Levene's test and, in case of significance at $p \leq 0.05$, we re-analyzed the data with the non-parametric Kruskal-Wallis ANOVA test at $p \leq 0.05$. We report effect size for ANOVA as omega-squared (ω^2) with 0.01, 0.06, and 0.14 considered small, medium and large effects (Field, 2013). We also assessed correlation between the TETRAS, FMS, TWSTRS scores, tremor onset and duration, and dystonia onset and duration for the DT group, with the MRS, DTI, and connectivity measures using Pearson's correlation at $p \leq 0.05$ with FDR corrections.

In Supplementary Figures, we also show the data for the pDT and TAWD groups separately as well as individual participant data and compared directly between the pDT and TAWD with *t*-test ($p \leq 0.05$) for all our metrics.

3. Results

The three groups did not differ in terms of age, sex, handedness, and number of participants. The ET group had significantly higher TETRAS score than the DT group for Activities of Daily Living (ADL), Performance (Perf), and Total, but the ET and DT groups did not differ for tremor onset and duration (Table 1).

3.1. Functional connectivity

Here, we assessed functional connectivity between pair of ROI of the tremor network that are anatomically connected (Fig. 1A). We found 3 pairs of ROI with significant main effect of Group (Fig. 1B–D): between the right lobule V and right dentate nucleus, between the left lobule V and left dentate nucleus, and between the left lobule VI and left dentate nucleus ($F(2, 45) = 5.37$, $p = 0.008$; $F(2, 45) = 3.59$, $p = 0.04$; $F(2, 45) = 4.56$, $p = 0.02$, respectively; effect size [CI]: 0.15 [0, 0.33], 0.10 [0, 0.27], 0.14 [0, 033], respectively). All pairs of ROI showed lower FC for ET than HV and DT who did not differ from each other and post-hoc *t*-test confirmed those observations ($p \leq 0.05$, FDR corrected).

We assessed correlation between each pair of ROI and the TETRAS-total, FMS and TWSTRS scores and for tremor onset and duration for each of the ET and DT groups, but found no significant correlation.

Thus, we found that brain connectivity was differentially impacted in the tremor network for the ET and DT groups.

3.2. DTI

Regarding FA (Fig. 2 and Table 2), the one-way ANOVA revealed five clusters with significant group main effect. Fig. 2A shows those brain areas and Fig. 2B–F shows FA for each group and participants as well as post hoc statistical effects. Those areas included the right and left middle cerebellar peduncle (MCP), two clusters along the left corticospinal tract (CST), and one cluster in the left red nucleus. Even though the red nucleus is a grey matter area, there are lots of fibers going through and around it (Milardi et al., 2016), thus FA values likely include white matter signal; the effects in red nucleus resemble those of MCP and CST (see below) and reinforce that point. Note that the cluster in the right MCP (Fig. 2A) overlapped with the MRS cerebellum ROI (Fig. 4B) by 98.5 % across participants (see overlaid rectangle in Fig. 2A over the right MCP). As can be seen in both cerebellar clusters FA was lower for the HV compared to the ET which was lower than the DT. FA in red nucleus and both CST clusters was lower for the HV compared to the ET and DT who did not differ from each other. Effect sizes ranged from 0.27 to 0.44 for those five ANOVA (Table 2).

Regarding MD (Fig. 3 and Table 3), the one-way ANOVA revealed ifive clusters with significant group main effect. Fig. 3A shows those brain areas and Fig. 3B–F shows MD for each group and participants as well as post hoc statistical effects. Those areas included the cerebellum (two in the left lobule V (labelled as 1 and 2) and one in the right lobule I-IV-V and right VI), and left CST. In the four clusters in the cerebellum ET and DT had both lower MD than HV and ET and DT did not differ from each other; although note that DT was lower than ET in the right cerebellum VI ($p = 0.048$). In the CST DT had higher MD than HV and ET who did not differ from each other. Effect sizes ranged from 0.27 to 0.31 for those eight ANOVA (Table 3).

We assessed correlation for each of the ET and DT groups between FA and MD with the TETRAS-total scores. We found no significant correlation with FA for ET or DT (all $p > 0.22$ and 0.45). For MD, we found significant negative correlation for ET in both clusters of the left cerebellum lobule V and in the right cerebellum lobule I-IV-V indicating that ET patients with lower MD had higher TETRAS scores (left lob. V (1) $r(14) = -0.59$, $p = 0.045$; left lob. V (2) $r(14) = -0.70$, $p = 0.024$; right lob. I-IV-V $r(14) = -0.62$, $p = 0.044$; FDR corrected). Thus, MD seem to have clinical significance for ET, as more severe tremor symptoms were accompanied by lower MD in the cerebellum. No correlation was significant for the DT group (all $p > 0.40$). We also did not find significant correlation with FMS, TWSTRS and tremor onset and duration (all $p > 0.32$).

3.3. MRS

Fig. 4A shows fitted MRS spectrum and Fig. 4B shows voxel location in the cerebellum for a typical HV participant.

As a preliminary step, we determined whether the GABA+/Cr, Glx/Cr, NAA/Cr, or Cho/Cr metabolites ratios correlated with tissue composition for grey and white matter (GM, WM) and CSF across all groups. We found no significant relationship (all $p > 0.10$ for all metabolites). Therefore, we used the metabolites ratios without correcting for tissue composition to avoid unnecessary data transformations.

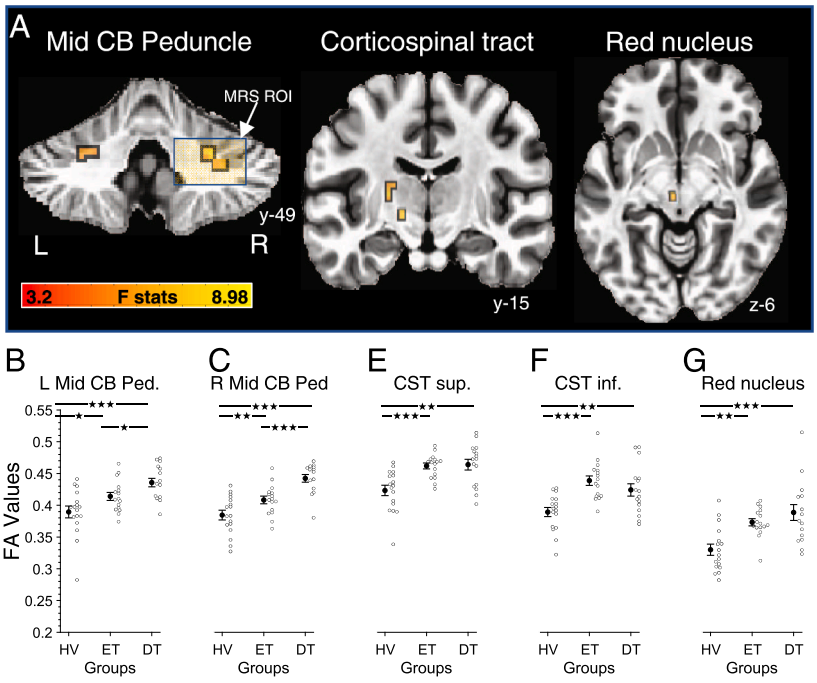

Fig. 2. Fractional anisotropy (FA). **A**: Brain areas with significant groups differences. **B-*G***: FA for brain areas shown in **A** for each group. Each cluster has a box around it to improve visualization. F stats represent the F statistics of the one-way ANOVA. Each datapoint represents one participant, and the means ± s.e.m. are reported. The box in **A** leftmost image represents the MRS ROI location. L-R: Left-Right, CB: cerebellum, CST: Corticospinal tract, Mid: middle, Ped: peduncle. r., radiata. * $p \leq 0.05$, ** $p \leq 0.01$, *** $p \leq 0.001$.

Table 2
Brain areas with group differences for Fractional anisotropy (FA).

Brain areas	MNI coordinates			Cluster Volume	F values		ω^2 [95 % CI]
	x	y	z	mm^3	Mean	Max	
R MCP	25	−49	−32	453	4.5	9.0	0.44 [0.21, 0.59]
L MCP	−28	−49	−32	219	3.9	5.9	0.26 [0.06, 0.44]
L CST sup.	−23	−14	8	125	4.4	6.3	0.27 [0.07, 0.45]
L Red nucleus	−5	−19	−7	31	5.2	5.2	0.29 [0.08, 0.47]
L CST inf.	−15	−14	−5	31	5.7	5.9	0.27 [0.06, 0.45]

MNI coordinates of brain areas with significant group main effects for FA. *F* values represent the *F* statistics of the ANOVA. Ω^2: Omega squared for effect size and 95% Confidence interval (CI). MCP: Middle Cerebellar Peduncle, CST: Corticospinal tract, sup: superior, inf: inferior. L-R: Left-Right.

Figure 4C-F shows the GABA/Cr, Glx/Cr, NAA/Cr, and Cho/Cr metabolites ratios for each group (means ± s.e.m.). For the GABA/Cr metabolite ratios the one-way ANOVA with HV, ET and DT groups revealed a trend towards a significant main effect of group ($F(2, 45) = 3.1$, $p = 0.054$, $\omega^2 = 0.08$) and post hoc contrasts revealed a trend towards a significantly lower GABA+/Cr ratio for the HV compared to the ET, as well as for the HV compared to the DT, while the ET and DT did not differ from each other ($p = 0.053, 0.053, 0.77$, respectively). For Glx/Cr, despite lower levels for the HV group compared to the ET and DT groups, the group main effect did not reach statistical significance ($F(2, 45) = 2.51$, $p = 0.09$, $\omega^2 = 0.06$). For NAA/Cr and Cho/Cr we found no significant main effects of groups ($F(2, 44) = 0.44 p = 0.65$, $\omega^2 = -0.02$ and $F(2, 43) = 2.60 p = 0.09$, $\omega^2 = 0.07$, respectively).

We determined that the MRS ROI in the cerebellum covered about 95 % of the dentate nucleus, 55–75 % of the interpositus nucleus, and 0 % of the fastigial nucleus across groups. Further, the dentate and interpositus nuclei contributed only 6 ± 1 % of the cerebellum ROI coverage, while grey and white matter contributed 74 ± 4 % and 21 ± 3 %, respectively. Therefore, the MRS signal comes mainly from the cerebellar hemisphere.

We also calculated Pearson correlation between the TETRAS-total, FMS and TWSTRS scores and tremor onset and duration with the metabolite ratios but found no significant correlation (all $p > 0.38$).

4. Discussion

We aimed to better understand the pathophysiology of ET and DT within the tremor network using multimodal neuroimaging with resting-state fMRI, DTI, and MRS. We found several areas withing the tremor network affected differently from the ET and DT diseases, with some areas showing elevated and others decreased metrics depending on their location.

In the cerebellar hemisphere, we found reduced MD, but elevated GABA + for ET and DT compared to HV. Findings present in both diseases might be related to the phenomenology, that is the tremor, and not necessarily its etiology. Also, in ET, but not DT, lower MD values were associated with higher TETRAS-total scores in three cerebellar regions (both left lob. V and right lob. I-IV-V, Fig. 3). These results likely relate to the neurodegeneration of the cerebellar hemisphere due to the PC loss but also to other changes such as GABAergic basket cells axonal hypertrophy (Louis and Faust, 2020a), axonal swelling and torpedos of PC (Louis et al., 2007; Louis, 2010), and synaptic pruning deficits in PC (Pan et al., 2020). However, which of these changes is specifically responsible for our results is beyond the current work. As MD measures water diffusivity in all directions and reflects microstructural alterations, reduced diffusivity could relate to an expansion of cells size aforesaid (e.g., axonal swelling and torpedos of PC). Since our MRS signal came mainly from the cerebellar cortex rather than the dentate nucleus, inhibitory interneurons (e.g., basket and stellate neurons) are likely the source of the elevated GABA. Purkinje cells are inhibitory also, but not likely to be responsible for increased GABA, since these cells are diminished in ET (Hartstone et al., 2020; Pan et al., 2020) and also in dystonia as suggested by a pathological study in cervical dystonia (Prudente et al., 2013). Prior work in ET found no GABA difference compared to controls (Louis et al., 2017; Tapper et al., 2020; Buijink et al., 2021), although one study reported the GABA+/Glx ratio correlated positively with tremor severity (Tapper et al., 2020). We did not find differences between ET and DT in GABA + which might relate to the

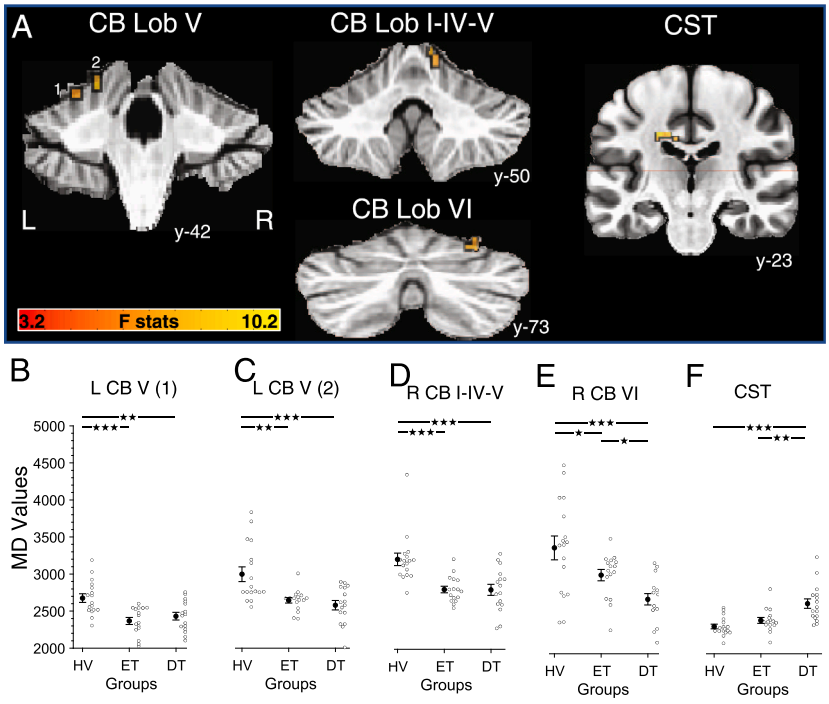

Fig. 3. Mean diffusivity (MD). **A**: Brain areas with significant groups differences. **B-I**: MD for brain areas shown in A for each group. Each cluster has a box around it to improve visualization. F stats represent the F statistics of the one-way ANOVA. Each datapoint represents one participant, and the means ± s.e.m. are reported. L-R: Left-Right, Lob: Lobule, g: gyrus, CST: Corticospinal tract, CB: cerebellum, Ant: anterior, r: radiation. * $p \leq 0.05$, ** $p \leq 0.01$, *** $p \leq 0.001$.

Table 3
Brain areas with group differences for Mean diffusivity (MD).

Brain areas	MNI coordinates			Cluster Volume	F values		ω^2 [95 % CI]
	x	y	z	mm^3	Mean	Max	
L CST	−20	−22	33	422	4.3	6.9	0.31 [0.10, 0.49]
R CB I V VI	8	−52	−12	125	5.2	6.1	0.31 [0.09, 0.48]
R CB VI	28	−72	−20	78	4.8	5.3	0.26 [0.06, 0.44]
L CB V (1)	−28	−44	−25	31	4.9	5.6	0.27 [0.06, 0.45]
L CB V (2)	−18	−42	−20	31	6.1	6.5	0.27 [0.06, 0.45]

MNI coordinates of brain areas with significant group main effects for MD. *F* values represent the *F* statistics of the one-way ANOVA. Ω^2: Omega squared for effect sized and 95% Confidence interval (CI). CST: Corticospinal tract, CB: cerebellum, L CB (1) and (2) refers to each cluster in Fig. 3. L-R: Left-Right.

presence of PC loss, and likely others neuronal changes, in each disease (Prudente et al., 2013; Hartstone et al., 2020; Pan et al., 2020).

We found no report of MRS studies in DT, and studies in pure dystonia (focal hand dystonia, cervical dystonia) showed mixed results: reduced GABA or reduced GABA binding in the cerebellum, sensorimotor cortex and other areas (Pollard et al., 2016; Gallea et al., 2018), while others report no GABA difference in basal ganglia and sensorimotor cortex (Herath et al., 2010). It is not possible to separate whether the GABA + differences in our dystonia cohort are due to the dystonia or the tremor, though the presence of similar changes in the ET group favors the tremor. We did not find group differences on Glx, NAA and Cho which could relate to our ROI that included cerebellar cortex, white matter, and dentate nucleus while others had measured these areas separately (Louis et al., 2002; Pagan et al., 2003). Surely more work is needed to decipher which metabolites in which region is affected in which disease. It is important to consider the MRS voxel selected for GABA study is of 18 ml, thus the cellular composition and balance within the area are at most speculative.

Connectivity between ROI in the tremor network was assessed with FC and DTI (FA, MD). FC analysis revealed decreased connectivity between the cerebellar hemispheres and dentate nucleus bilaterally for the ET compared to the DT and HV groups who did not differ from each other. This reduced FC is likely to relate to the above-mentioned changes in the cerebellar hemisphere which projects to the dentate nucleus. Those results corroborate prior studies reporting decreased connectivity in ET (Neely et al., 2014; Benito-León et al., 2015; Buijink et al., 2015; Fang et al., 2015; Gallea et al., 2015; Mueller et al., 2017; Roy et al., 2018; Benito-Leon et al., 2019; DeSimone et al., 2019; Nicoletti et al., 2020; Tikoo et al., 2020). The lower FC for ET compared to DT would suggest that the neurodegenerative changes in each disease are different, despite implicating PC loss (Prudente et al., 2013; Hartstone et al., 2020; Pan et al., 2020). But it remains somewhat puzzling that we did not find other FC differences in the tremor network.

We also found that FA in the MCP bilaterally, along the CST and red nucleus was elevated for ET and DT. Further, we found higher FA for DT compared to ET in the MCP bilaterally. This elevated activity along the tremor network is probably due to elevated tremulous activity within the tremor network ROI and as such increased communication along its pathway. The neuronal dysfunctions in the cerebellar hemisphere changes would enhance inhibition in the dentate nucleus and allow for the motor network to be overactive causing tremor (Paris-Robidas et al., 2011). Elevated FA in MCP and CST thus seems in line with the hyperkinetic nature of the ET and DT disorders. Prior work in dystonia have reported involvement of the cerebellum (Prudente et al., 2013; Sharma, 2019), and thus since DT is a combination of dystonia and tremor could explain the elevated FA for DT. Relatedly, the CST also showed impairments for ET and DT with elevated MD, as well as elevated FA. Elevated MD and FA indicate higher diffusivity, and this suggests anatomical changes along the CST of an overactive tremor network.

It may seem incongruous that we found higher FA values in ET and DT as FA assesses water diffusivity along white matter tracts and is a measure of axonal integrity, with lower values typically associated with

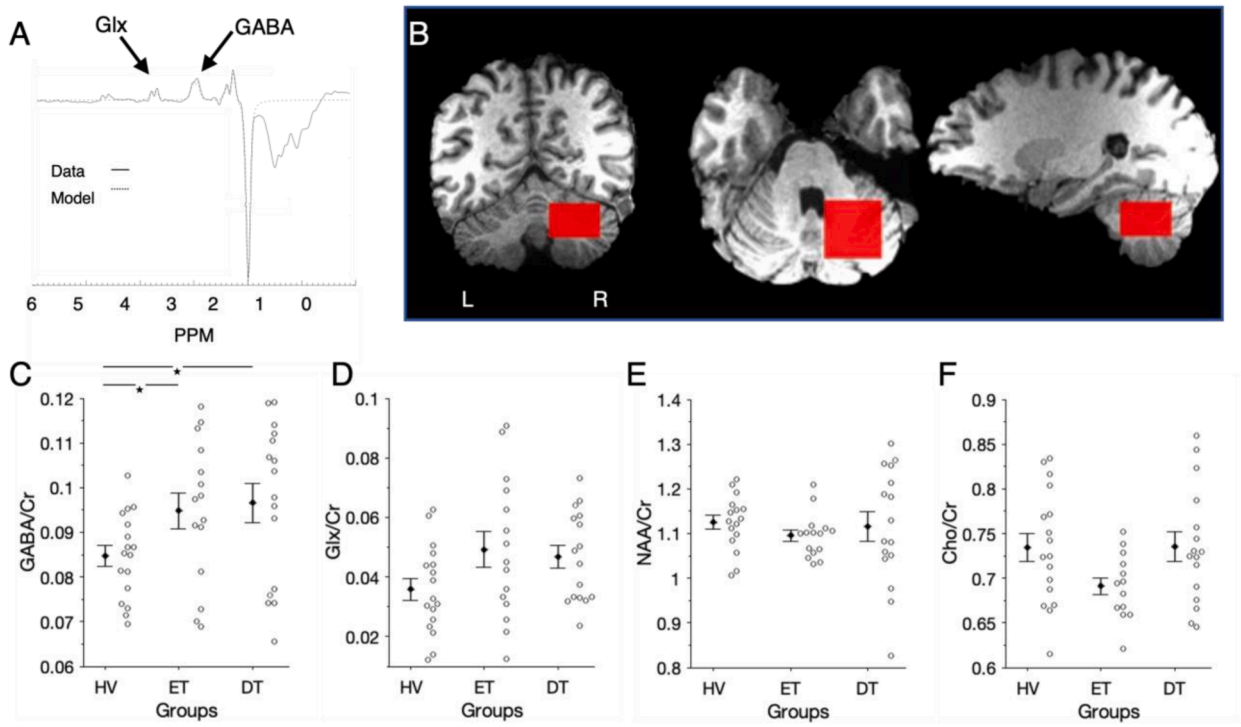

Fig. 4. Magnetic Resonance Spectroscopy (MRS). **A**: MRS spectra for a typical participant. **B**: ROI location in the right cerebellum for a HV participant. **C-F**: Cerebellar concentration of metabolite GABA+/Cr, Glx/Cr, NAA/Cr, Cho/Cr. Each datapoint represents one participant, and the means ± s.e.m. are reported. L-R: Left-Right. Glx: glutamate/glutamine, NAA: *N*-Acetylaspartate, Cho: choline, Cr: creatine. * $p \leq 0.05$.

ET and other diseases (Cerasa et al., 2014; Tae et al., 2018). This would support that neither ET nor DT are white matter diseases. In that sense, the increased FA might simply reflect overused pathways.

Only recently have some studies assessed separately DT and ET. A study compared spasmodic dysphonia patients with and without dystonic tremor of voice and showed largely overlapping connectivity results (Battistella and Simonyan, 2019) while Desimone et al. (2019) studied cervical dystonic patients with head tremor and reported reduced functional connectivity for ET and dystonic patients compared to controls, but even more reduced connectivity in dystonic patients than ET across cerebellar, basal ganglia, and cortical areas. Here, our DT group was composed of patients with cervical dystonia and writer's cramp all having hand tremor and we did not find differences in the tremor network compared to HV. At first sight, the various DT phenotypes also have different connectivity patterns and most likely task-related brain activation which reflect the heterogeneity of the dystonia disorder with or without accompanying tremor; also consider that these studies all used different methods.

Limitations in the current study include a relatively low number of participants, which may explain the null results with Glx, Cho, and NAA, although the number of participants is in the same range as similar prior work with ET, DT, and HV groups (Kirke et al., 2017; Battistella and Simonyan, 2019; DeSimone et al., 2019; Hess et al., 2020). For MRS, our ROI included part of the cerebellar cortex, white matter, and almost all the dentate nucleus preventing a separate estimation of each area's contribution to ET and DT. It remains puzzling why we found no MRS difference in the cerebellum between DT and ET, while we found higher TETRAS scores for ET than DT. Clinical severity between the DT and ET groups was not matched on the TETRAS scores as DT and ET differ in their pathophysiology and TETRAS was designed specifically for ET. Nevertheless, this could have influenced some of our metrics.

In Supplementary figures, as mentioned above, we presented individual participant data for the pDT and TAWD groups separately to show that the two sub-groups overlapped considerably, and the statistical analysis confirmed that there were no group differences. Thus, the null results of no group difference are likely not due to power issues, at least with the metrics of our study. In all, within the confine of our measurements, we did not find differences between pDT and TAWD.

In summary, we assessed differences between patients with ET and DT with multi-modal neuroimaging. We show that ET and DT differ from one another on DTI and functional connectivity measurements in the cerebellum and tremor network, although we found no difference with MRS. Thus, this reinforces the use of multimodal imaging to understand the pathophysiology of these diseases and better diagnose these patients. Tremor is a common movement disorder that can be accompanied with dystonia, but it remains challenging to dissociate these as no biomarker exists. Our MRI data as well as neurophysiological data (Panyakaew et al., 2020) indicate that such differences can be found. Future work in this direction should ease the diagnosis and possibly treatment of those patients.

Declaration of Competing Interest

The authors declare that they have no known competing financial interests or personal relationships that could have appeared to influence the work reported in this paper.

Data availability

Data would be available upon request and IRB authorization

Acknowledgements

This project was supported by the NINDS Intramural Research Program. Authors thank JW van der Veen for the MRS scripts and support.

Funding

This work was supported by the Intramural Research Program of the National Institute of Neurological Disorders and Stroke, National

Institutes of Health.

Appendix A. Supplementary data

Supplementary data to this article can be found online at https://doi.org/10.1016/j.nicl.2022.103247.

References

Albanese, A., Bhatia, K., Bressman, S.B., Delong, M.R., Fahn, S., Fung, V.S., Hallett, M., Jankovic, J., Jinnah, H.A., Klein, C., Lang, A.E., Mink, J.W., Teller, J.K., 2013. Phenomenology and classification of dystonia: a consensus update. Mov Disord 28, 863–873.

Battistella, G., Simonyan, K., 2019. Top-down alteration of functional connectivity within the sensorimotor network in focal dystonia. Neurology 92, e1843 e1851.

Benito-León, J., Louis, E.D., Romero, J.P., Hernández-Tamames, J.A., Manzanedo, E., Álvarez-Linera, J., Bermejo-Pareja, F., Posada, I., Rocon, E., 2015. Altered Functional Connectivity in Essential Tremor. Medicine 94, e1936.

Benito-Leon, J., Sanz-Morales, E., Melero, H., Louis, E.D., Romero, J.P., Rocon, E., Malpica, N., 2019. Graph theory analysis of resting-state functional magnetic resonance imaging in essential tremor. Hum Brain Mapp 40, 4686–4702.

Benjamini, Y., Hochberg, Y., 1995. Controlling the False Discovery Rate: A Practical and Powerful Approach to Multiple Testing. Journal of the Royal Statistical Society: Series B (Methodological) 57, 289–300.

Bhatia KP, Bain P, Bajaj N, Elble RJ, Hallett M, Louis ED, Raethjen J, Stamelou M, Testa CM, Deuschl G, Tremor Task Force of the International P, Movement Disorder S (2018) Consensus Statement on the classification of tremors. from the task force on tremor of the International Parkinson and Movement Disorder Society. Mov Disord 33:75-87.

Bottomley, P.A., 1984. NMR in medicine. Computerized Radiology 8, 57–77.

Bottomley, P.A., 1987. Spatial Localization in NMR Spectroscopy in Vivo. Annals of the New York Academy of Sciences 508, 333–348.

Bove, F., Di Lazzaro, G., Mulas, D., Cocciolillo, F., Di Giuda, D., Bentivoglio, A.R., 2018. A role for accelerometry in the differential diagnosis of tremor syndromes. Funct Neurol 33, 45–49.

Buijink, A.W.G., van der Stouwe, A.M.M., Broersma, M., Sharifi, S., Groot, P.F.C., Speelman, J.D., Maurits, N.M., van Rootselaar, A.-F., 2015. Motor network disruption in essential tremor: a functional and effective connectivity study. Brain 138, 2934–2947.

Buijink, A.W.G., Prent, N., Puts, N.A., Schrantee, A., Potters, W.V., van Rootselaar, A.F., 2021. GABA, Glutamate, and NAA Levels in the Deep Cerebellar Nuclei of Essential Tremor Patients. Front Neurol 12, 664735.

Cerasa, A., Quattrone, A., 2016. Linking Essential Tremor to the Cerebellum—Neuroimaging Evidence. The Cerebellum 15, 263–275.

Cerasa, A., Nisticò, R., Salsone, M., Bono, F., Salvino, D., Morelli, M., Arabia, G., Quattrone, A., 2014. Neuroanatomical correlates of dystonic tremor: A cross-sectional study. Parkinsonism & Related Disorders 20, 314–317.

Cox, R.W., 1996. AFNI: Software for Analysis and Visualization of Functional Magnetic Resonance Neuroimages. Computers and Biomedical Research 29, 162–173.

DeSimone, J.C., Archer, D.B., Vaillancourt, D.E., Wagle Shukla, A., 2019. Network-level connectivity is a critical feature distinguishing dystonic tremor and essential tremor. Brain 142, 1644–1659.

Deuschl, G., Bain, P., Brin, M., 1998. Consensus statement of the Movement Disorder Society on Tremor. Ad Hoc Scientific Committee. Mov Disord 13 (Suppl 3), 2–23.

Fang, W., Chen, H., Wang, H., Zhang, H., Puneet, M., Liu, M., Lv, F., Luo, T., Cheng, O., Wang, X., Lu, X., 2015. Essential tremor is associated with disruption of functional connectivity in the ventral intermediate Nucleus-Motor Cortex-Cerebellum circuit. Human Brain Mapping 37, 165–178.

Field, A., 2013. Discovering statistics using IBM SPSS statistics, 4th edn. SAGE, London.

Gallea, C., Popa, T., García-Lorenzo, D., Valabregue, R., Legrand, A.-P., Marais, L., Degos, B., Hubsch, C., Fernández-Vidal, S., Bardinet, E., Roze, E., Lehéricy, S., Vidailhet, M., Meunier, S., 2015. Intrinsic signature of essential tremor in the cerebello-frontal network. Brain 138, 2920–2933.

Gallea, C., Herath, P., Voon, V., Lerner, A., Ostuni, J., Saad, Z., Thada, S., Solomon, J., Horovitz, S.G., Hallett, M., 2018. Loss of inhibition in sensorimotor networks in focal hand dystonia. NeuroImage: Clinical 17, 90–97.

Geramita, M., van der Veen, J.W., Barnett, A.S., Savostyanova, A.A., Shen, J., Weinberger, D.R., Marenco, S., 2011. Reproducibility of prefrontal γ-aminobutyric acid measurements with J -edited spectroscopy. NMR in Biomedicine 24, 1089–1098.

Hartstone, W.G., Brown, M.H., Kelly, G.C., Tate, W.J., Kuo, S.H., Dwork, A.J., Louis, E.D., Faust, P.L., 2020. Dentate Nucleus Neuronal Density: A Postmortem Study of Essential Tremor Versus Control Brains. Movement Disorders 36, 995–999.

Haubenberger, D., Hallett, M., 2018. Essential Tremor. N Engl J Med 378, 1802–1810.

Herath, P., Gallea, C., van der Veen, J.W., Horovitz, S.G., Hallett, M., 2010. In vivo neurochemistry of primary focal hand dystonia: a magnetic resonance spectroscopic neurometabolite profiling study at 3T. Mov Disord 25, 2800–2808.

Hess, C.W., Gatto, B., Chung, J.W., Ho, R.L.M., Wang, W.-e., Wagle Shukla, A., Vaillancourt, D.E., 2020. Cortical Oscillations in Cervical Dystonia and Dystonic Tremor. Cerebral Cortex. Communications 1.

Irfanoglu, M.O., Nayak, A., Jenkins, J., Hutchinson, E.B., Sadeghi, N., Thomas, C.P., Pierpaoli, C., 2016. DR-TAMAS: Diffeomorphic Registration for Tensor Accurate Alignment of Anatomical Structures. NeuroImage 132, 439–454.

Jedynak, C.P., Bonnet, A.M., Agid, Y., 1991. Tremor and idiopathic dystonia. Mov Disord 6, 230–236.

Jinnah, H.A., Neychev, V., Hess, E.J., 2017. The Anatomical Basis for Dystonia: The Motor Network Model. Tremor and Other Hyperkinetic Movements 7, 506.

Jo, H.J., Saad, Z.S., Simmons, W.K., Milbury, L.A., Cox, R.W., 2010. Mapping sources of correlation in resting state FMRI, with artifact detection and removal. NeuroImage 52, 571–582.

Kirke, D.N., Battistella, G., Kumar, V., Rubien-Thomas, E., Choy, M., Rumbach, A., Simonyan, K., 2017. Neural correlates of dystonic tremor: a multimodal study of voice tremor in spasmodic dysphonia. Brain Imaging and Behavior 11, 166–175.

Lehéricy, S., Tijssen, M.A.J., Vidailhet, M., Kaji, R., Meunier, S., 2013. The anatomical basis of dystonia: Current view using neuroimaging. Movement Disorders 28, 944–957.

Louis, E.D., 2010. Essential tremor: evolving clinicopathological concepts in an era of intensive post-mortem enquiry. The Lancet Neurology 9, 613–622.

Louis, E.D., Faust, P.L., Vonsattel, J.P.G., Honig, L.S., Rajput, A., Robinson, C.A., Rajput, A., Pahwa, R., Lyons, K.E., Ross, G.W., Borden, S., Moskowitz, C.B., Lawton, A., Hernandez, N., 2007. Neuropathological changes in essential tremor: 33 cases compared with 21 controls. Brain 130, 3297–3307.

Louis, E.D., Faust, P.L., 2020a. Essential tremor pathology: neurodegeneration and reorganization of neuronal connections. Nature Reviews Neurology 16, 69–83.

Louis, E.D., Faust, P.L., 2020b. Essential tremor: the most common form of cerebellar degeneration? Cerebellum Ataxias 7, 12.

Louis, E.D., Shungu, D.C., Chan, S., Mao, X., Jurewicz, E.C., Watner, D., 2002. Metabolic abnormality in the cerebellum in patients with essential tremor: a proton magnetic resonance spectroscopic imaging study. Neuroscience Letters 333, 17–20.

Louis, E.D., Hernandez, N., Dyke, J.P., Ma, R.E., Dydak, U., 2017. In Vivo Dentate Nucleus Gamma-aminobutyric Acid Concentration in Essential Tremor vs. Controls. The Cerebellum 17, 165–172.

Milardi, D., Cacciola, A., Cutroneo, G., Marino, S., Irrera, M., Cacciola, G., Santoro, G., Ciolli, P., Anastasi, G., Calabro, R.S., Quartarone, A., 2016. Red nucleus connectivity as revealed by constrained spherical deconvolution tractography. Neuroscience Letters 626, 68–73.

Mueller, K., Jech, R., Hoskovcová, M., Ulmanová, O., Urgošík, D., Vymazal, J., Růžička, E., 2017. General and selective brain connectivity alterations in essential tremor: A resting state fMRI study. NeuroImage: Clinical 16, 468–476.

Neely, K.A., Kurani, A.S., Shukla, P., Planetta, P.J., Wagle Shukla, A., Goldman, J.G., Corcos, D.M., Okun, M.S., Vaillancourt, D.E., 2014. Functional Brain Activity Relates to 0–3 and 3–8 Hz Force Oscillations in Essential Tremor. Cerebral Cortex 25, 4191–4202.

Nicoletti, V., Cecchi, P., Pesaresi, I., Frosini, D., Cosottini, M., Ceravolo, R., 2020. Cerebello-thalamo-cortical network is intrinsically altered in essential tremor: evidence from a resting state functional MRI study. Scientific Reports 10.

Pagan, F.L., Butman, J.A., Dambrosia, J.M., Hallett, M., 2003. Evaluation of essential tremor with multi-voxel magnetic resonance spectroscopy. Neurology 60, 1344–1347.

Pan, M.-K., Li, Y.-S., Wong, S.-B., Ni, C.-L., Wang, Y.-M., Liu, W.-C., Lu, L.-Y., Lee, J.-C., Cortes, E.P., Vonsattel, J.-P.-G., Sun, Q., Louis, E.D., Faust, P.L., Kuo, S.-H., 2020. Cerebellar oscillations driven by synaptic pruning deficits of cerebellar climbing fibers contribute to tremor pathophysiology. Science Translational Medicine 12, eaay1769.

Pandey, S., Sarma, N., 2016. Tremor in dystonia. Parkinsonism & Related Disorders 29, 3–9.

Panyakaew, P., Cho, H.J., Lee, S.W., Wu, T., Hallett, M., 2020. The Pathophysiology of Dystonic Tremors and Comparison With Essential Tremor. J Neurosci 40, 9317–9326.

Paris-Robidas, S., Brochu, E., Sintes, M., Emond, V., Bousquet, M., Vandal, M., Pilote, M., Tremblay, C., Di Paolo, T., Rajput, A.H., Rajput, A., Calon, F., 2011. Defective dentate nucleus GABA receptors in essential tremor. Brain 135, 105–116.

Paris-Robidas, S., Brochu, E., Sintes, M., Emond, V., Bousquet, M., Vandal, M., Pilote, M., Tremblay, C., Di Paolo, T., Rajput, A.H., Rajput, A., Calon, F., 2012. Defective dentate nucleus GABA receptors in essential tremor. Brain 135, 105–116.

Pfefferbaum, A., Adalsteinsson, E., Rohlfing, T., Sullivan, E.V., 2010. Diffusion tensor imaging of deep gray matter brain structures: effects of age and iron concentration. Neurobiol Aging 31, 482–493.

Pierpaoli C. WL, Irfanoglu M. O., Barnett A., Basser P., Chang L-C, Koay C., Pajevic S., Rohde G., Sarlls J., Wu M. (2010) TORTOISE: an integrated software package for processing of diffusion MRI data, ISMRM 18th annual meeting, Stockholm, Sweden, abstract #1597.

Pollard, R., Shelton, E., Koo, P., Berman, B., 2016. GABA-A receptor binding is abnormal in cervical dystonia (P1.030). Neurology 86, P1 .030.

Prudente, C.N., Pardo, C.A., Xiao, J., Hanfelt, J., Hess, E.J., LeDoux, M.S., Jinnah, H.A., 2013. Neuropathology of cervical dystonia. Experimental Neurology 241, 95–104.

R Core Team, 2021. R: A language and environment for statistical computing. R Foundation for Statistical Computing, Vienna, Austria https://www.R-project.org/. In.

Rothman, D.L., Petroff, O.A., Behar, K.L., Mattson, R.H., 1993. Localized 1H NMR measurements of gamma-aminobutyric acid in human brain in vivo. Proc Natl Acad Sci U S A 90, 5662–5666.

Roy, A., Coombes, S.A., Chung, J.W., Archer, D.B., Okun, M.S., Hess, C.W., Wagle Shukla, A., Vaillancourt, D.E., 2018. Cortical dynamics within and between parietal and motor cortex in essential tremor. Movement Disorders 34, 95–104.

Rudzińska, M., Krawczyk, M., Wójcik-Pędziwiatr, M., Szczudlik, A., Wasielewska, A., 2013. Tremor associated with focal and segmental dystonia. Neurologia i Neurochirurgia Polska 47, 223–231.

Sedov, A., Usova, S., Semenova, U., Gamaleya, A., Tomskiy, A., Beylergil, S.B., Jinnah, H. A., Shaikh, A.G., 2020. Pallidal Activity in Cervical Dystonia with and Without Head Tremor. The Cerebellum 19, 409–418.
Shaikh, A.G., Jinnah, H.A., Tripp, R.M., Optican, L.M., Ramat, S., Lenz, F.A., Zee, D.S., 2008. Irregularity distinguishes limb tremor in cervical dystonia from essential tremor. Journal of Neurology, Neurosurgery & Psychiatry 79, 187–189.
Shaikh, A.G., Zee, D.S., Jinnah, H.A., 2015. Oscillatory head movements in cervical dystonia: Dystonia, tremor, or both? Movement Disorders 30, 834–842.
Sharma, N., 2019. Neuropathology of Dystonia. Tremor Other Hyperkinet Mov (N Y) 9, 569.
Smith, S.M., Nichols, T.E., 2009. Threshold-free cluster enhancement: addressing problems of smoothing, threshold dependence and localisation in cluster inference. Neuroimage 44, 83–98.
Tae, W.-S., Ham, B.-J., Pyun, S.-B., Kang, S.-H., Kim, B.-J., 2018. Current Clinical Applications of Diffusion-Tensor Imaging in Neurological Disorders. Journal of Clinical Neurology 14, 129.
Tapper, S., Göransson, N., Lundberg, P., Tisell, A., Zsigmond, P., 2020. A pilot study of essential tremor: cerebellar GABA+/Glx ratio is correlated with tremor severity. Cerebellum & Ataxias 7.
Taylor, P.A., Saad, Z.S., 2013. FATCAT: (An Efficient) Functional And Tractographic Connectivity Analysis Toolbox. Brain Connectivity 3, 523–535.
Tikoo, S., Pietracupa, S., Tommasin, S., Bologna, M., Petsas, N., Bharti, K., Berardelli, A., Pantano, P., 2020. Functional disconnection of the dentate nucleus in essential tremor. Journal of Neurology 267, 1358–1367.
Tinaz, S., Belluscio, B.A., Malone, P., van der Veen, J.W., Hallett, M., Horovitz, S.G., 2014. Role of the sensorimotor cortex in Tourette syndrome using multimodal imaging. Hum Brain Mapp 35, 5834–5846.